

REPORT DOCUMENTATION PAGE			Form Approved OMB No. 0704-0188	
<small>Public reporting burden for this collection of information is estimated to average 1 hour per response, including the time for reviewing instructions, searching existing data sources, gathering and maintaining the data needed, and completing and reviewing the collection of information. Send comments regarding this burden estimate or any other aspect of this collection of information, including suggestions for reducing this burden, to Washington Headquarters Services, Directorate for Information Operations and Reports, 1215 Jefferson Davis Highway, Suite 1204, Arlington, VA 22202-4302, and to the Office of Management and Budget, Paperwork Reduction Project (0704-0188), Washington, DC 20503.</small>				
1. AGENCY USE ONLY (Leave blank)	2. REPORT DATE January 25, 1996	3. REPORT TYPE AND DATES COVERED preprint of journal article		
4. TITLE AND SUBTITLE Structures and Molecular Surface Electrostatic Potentials of High Denisty C, N, H Systems		5. FUNDING NUMBERS N00014-95-1-0028 Dr. Richard S. Miller R&T Code 33e 1806		
6. AUTHOR(S) Jane S. Murray, Richard Gildardi, M. Edward Grice, Pat Lane and Peter Politzer				
7. PERFORMING ORGANIZATION NAME(S) AND ADDRESS(ES) University of New Orleans Department of Chemistry New Orleans, Louisiana 70148		8. PERFORMING ORGANIZATION REPORT NUMBER 89		
9. SPONSORING/MONITORING AGENCY NAME(S) AND ADDRESS(ES) Office of Naval Research Code 333 800 N. Quincy Street Arlington, VA 22217		10. SPONSORING/MONITORING AGENCY REPORT NUMBER		
11. SUPPLEMENTARY NOTES				
12a. DISTRIBUTION/AVAILABILITY STATEMENT Approved for public release. Unlimited distribution.		12b. DISTRIBUTION CODE 19960208 081		
13. ABSTRACT (Maximum 200 words) Tri-s-triazine and two ditetrazolodiazines are known to have unusually high crystal densities (for unsubstituted C, N, H compounds). We have used a nonlocal density functional procedure to compute the geometries and energies of these and three related molecules, and then calculated the <i>ab initio</i> SCF electrostatic potentials on their molecular surfaces. We attribute the high densities to the relatively small molecular volumes and the strong intermolecular attractions arising from highly varying surface potentials. The energy differences of the two ditetrazoles and their diazide tautomers were computed, as well as for the dinitro derivative of one of the former.				
14. SUBJECT TERMS high denisty compounds; tri-s-triazine; ditetrazolodiazines; diazides; high-nitrogen compounds; surface electrostatic potential		15. NUMBER OF PAGES 18		
		16. PRICE CODE		
17. SECURITY CLASSIFICATION OF REPORT Unclassified	18. SECURITY CLASSIFICATION OF THIS PAGE Unclassified	19. SECURITY CLASSIFICATION OF ABSTRACT Unclassified	20. LIMITATION OF ABSTRACT Unlimited	

OFFICE OF NAVAL RESEARCH

CONTRACT N00014-95-1-0028

R&T Code 4131D02

Dr. Richard S. Miller

Technical Report No. 89

Structures and Molecular Surface Electrostatic Potentials
of High-Density C, N, H Systems

by

Jane S. Murray, Richard Gilardi, M. Edward Grice, Pat Lane and Peter Politzer

Prepared for Publication

in

Structural Chemistry

Department of Chemistry
University of New Orleans
New Orleans, LA 70148

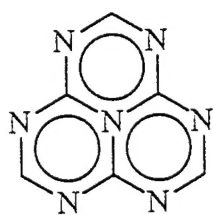
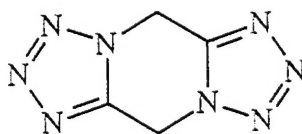
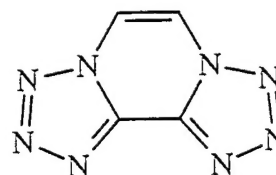
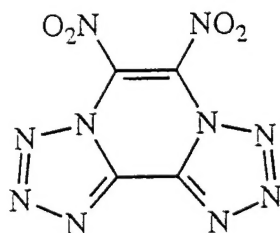
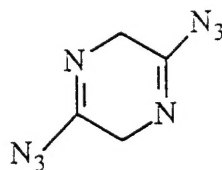
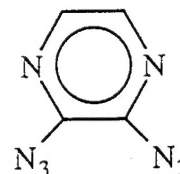
January 25, 1996

Reproduction in whole or in part is permitted for any purpose of the United States Government.

This document has been approved for public release and sale; its distribution is unlimited.

Introduction

Since the detonation performance of an energetic material is directly related to its density [1], the latter property is an important criterion in evaluating prospective energetic compounds. To the best of our knowledge, the crystalline forms of **1** - **3** have the highest densities that have been measured for any unsubstituted C, N, H compounds: **1**: 1.69 g/cm³ [2]; **2**: 1.715 g/cm³ [3]; **3**: 1.674 g/cm³ [4]. It is accordingly interesting to consider these as possible starting points for energetic molecules such as **4**, the dinitro derivative of **3**. In this context, a potential concern in the cases of **2** and **3** would be any tendency to rearrange to the azides **5** and **6** [5-12]. This point shall be addressed. However **1** - **3** do exist and form stable crystalline materials. It should be useful to investigate some of the properties of these molecules, and simultaneously to try to gain some insight into the reasons for their high crystal densities. With these objectives, we have computed and analyzed their molecular electrostatic potentials, as well as those of **4** - **6**.

**1****2****3****4****5****6**

Methods and Procedure

The electrostatic potential $V(\mathbf{r})$ created at any point \mathbf{r} by the nuclei and electrons of a molecule is defined rigorously by eq. (1).

$$V(\mathbf{r}) = \sum_A \frac{Z_A}{|\mathbf{R}_A - \mathbf{r}|} - \int \frac{\rho(\mathbf{r}') d\mathbf{r}'}{|\mathbf{r}' - \mathbf{r}|} \quad (1)$$

Z_A is the charge on nucleus A, located at \mathbf{R}_A , and $\rho(\mathbf{r})$ is the electronic density, which we obtain from the molecular wave function. $V(\mathbf{r})$ is a real physical property, which can be determined

experimentally, by diffraction methods, as well as computationally [13]. It has proven to be a useful tool for predicting and interpreting molecular interactive behavior [13-15]. Regions of positive and negative potential on the molecular surface, defined as the 0.001 electron/bohr³ contour of $\rho(\mathbf{r})$ [16], are indicative of sites attractive to nucleophiles and electrophiles, respectively.

In recent years, we have developed more quantitative methods for using the electrostatic potential to analyze non-covalent molecular interactions [17-21]. We have introduced several statistically-based indices that are defined in terms of the surface potential, two of which are presented in eqs. (2) and (3).

$$\Pi = \frac{1}{n} \sum_{i=1}^n |V(\mathbf{r}_i) - \bar{V}_s| \quad (2)$$

$$\sigma_{\text{tot}}^2 = \sigma_+^2 + \sigma_-^2 = \frac{1}{m} \sum_{i=1}^m [V^+(\mathbf{r}_i) - \bar{V}_s^+]^2 + \frac{1}{n} \sum_{j=1}^n [V^-(\mathbf{r}_j) - \bar{V}_s^-]^2 \quad (3)$$

In these equations, $V(\mathbf{r}_i)$ is the value of $V(\mathbf{r})$ at point \mathbf{r}_i on the surface, and \bar{V}_s is the average value of the potential on the surface. In a similar fashion, $V^+(\mathbf{r}_i)$ and $V^-(\mathbf{r}_i)$ are the positive and negative values of $V(\mathbf{r})$ on the surface, and \bar{V}_s^+ and \bar{V}_s^- are their averages: $\bar{V}_s^+ = \frac{1}{m} \sum_{i=1}^m V^+(\mathbf{r}_i)$ and $\bar{V}_s^- = \frac{1}{n} \sum_{j=1}^n V^-(\mathbf{r}_j)$.

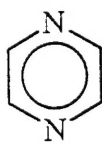
Π , given by eq. (2), is the average deviation of the electrostatic potential on the molecular surface. We have shown that Π is an effective measure of local polarity (or charge separation), which may be quite significant even in a molecule having zero dipole moment, e.g. CO₂ and *p*-dinitrobenzene [17]. The total variance, σ_{tot}^2 , given by eq. (3), is a measure of the spread of the values of the surface potential, and is particularly sensitive to positive and negative extrema [18,21].

In this work, molecular geometries and energies were computed with a nonlocal density functional procedure (GAUSSIAN 92/DFT [22], Becke exchange and Lee, Yang and Parr correlation functionals [23,24], 6-31G** basis set). Using these structures, the electrostatic potentials and related quantities were calculated at the *ab initio* HF/STO-5G level, in order that they be compatible with such data obtained earlier for other molecules [17,20,18,19,21,25]. We have shown that the resulting trends in the surface electrostatic potentials are the same when the HF/6-31G* basis set is used [26].

Results

Energies and structural data are shown in Table 1. There is overall satisfactory agreement between the calculated (gas phase) and experimentally-determined (crystalline) bond lengths for **1** - **3**. An interesting feature of **1** is the near-constancy of the bond lengths around its perimeter, contrasted to the considerably longer internal C-N bonds.

The surface electrostatic potentials of **1** - **6** are shown in Figures 1 - 5. Their dominant features are the extensive positive regions above the heterocyclic rings. (Note, in Table 2, the values of $V_{S,max}$, the most positive surface potentials.) Formally, all of these molecules are unsaturated and thus are expected to have pi electrons above the rings; in the case of benzene, for example, these produce a negative potential of -10.5 kcal/mole above the ring [27]. However analogous negative regions are not found in **1** - **6**, because of the effect of the strongly electron-attracting ring nitrogens; this has already been observed earlier for azines (e.g. **7** - **10**) [27,28]. The electron-withdrawing NO_2 groups in **4** cause the ring system to become even more positive (Figure 3b and Table 2).

**7****8****9****10**

The ring nitrogens on the peripheries of **1** - **6** have negative potentials of varying strengths associated with their lone pairs. In Tables 2 and 3 are listed their most negative values on the molecular surfaces, $V_{S,min}(N)$, and also in three-dimensions, $V_{min}(N)$. The triply-coordinated nitrogens in the central portions of the molecules have no negative potentials at all. The peripheral nitrogens accordingly have some basic character and some hydrogen-bond-accepting tendencies, although relatively weak; among the known compounds **1** - **3**, the strongest in both respects should be **1**, for which the present results combined with our earlier correlations [29,30] suggest a pK_a of about 0.0 and a hydrogen-bonding ability similar to that of pyrazine, **7**. It might have been anticipated that **1** will be similar to *s*-triazine (**8**) in these properties, but the negative potentials in **1** are actually stronger than in **8**; e.g. $V_{min}(N)$ is -80.0 kcal/mole in the former and -74.6 kcal/mole in the latter [28]. This is presumably because the peripheral nitrogens in **1** withdraw some electronic charge from the one in the center of the molecule, which is formally positive. The least basic ring nitrogens, overall, are those in **4**, which have lost a portion of their electronic charge to the nitro groups.

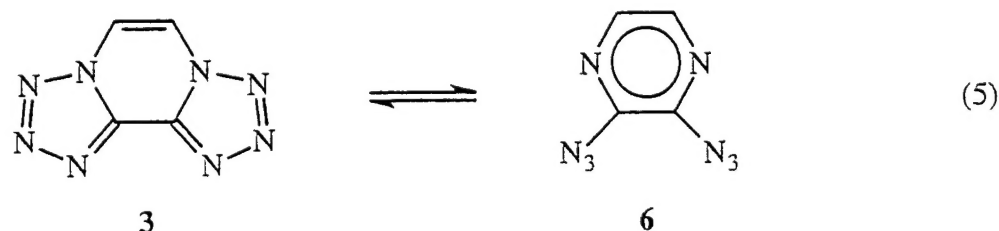
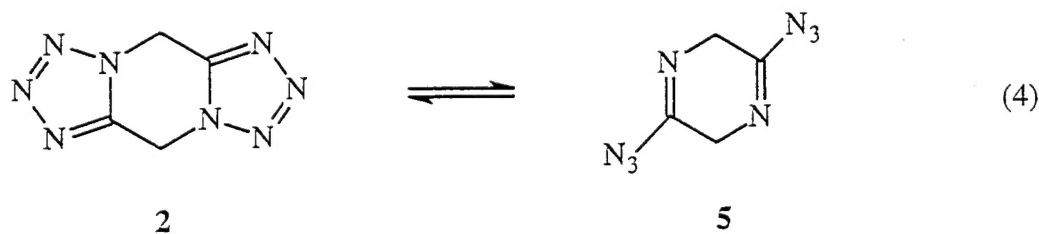
Table 2 also contains the calculated areas and volumes of **1** - **4**, based on the 0.001 au contour of the electronic density, as well as several properties computed from the surface

electrostatic potentials: Π , σ_+^2 , σ_-^2 and σ_{tot}^2 . The Π values of **1** - **4** show that these molecules have high degrees of internal charge separation, as can also be seen in Figures 1 - 3. For **1** - **4**, Π ranges from 21 to 25 kcal/mole, although we have usually found it to be between 2 and 15 kcal/mole for organic molecules [17]. **1** - **4** are good examples of how local polarity, as measured by Π , may differ from net overall polarity, given by the dipole moment. **1** and **2** have high values of Π , even though their dipole moments are zero, due to symmetry. Both **3** and **4** have non-zero dipole moments, but that of **3** is much larger, 6.12 vs. 1.24 Debyes at the HF/STO-5G//HF/3-21G level; this is because the polarity of the NO_2 groups in **4** is opposite in direction to that of the ring nitrogens. However the Π values of **3** and **4** are nearly the same (Table 2).

The magnitudes of σ_{tot}^2 are also large, between 238 and 354 (kcal/mole)² for **1** - **3**, and 423 (kcal/mole)² for **4**, whereas we usually find it to be below 180 (kcal/mole)² [18,19]. The high values of σ_{tot}^2 for **1** - **4** suggest strong electrostatic interaction tendencies. Although Figures 1 - 3a show that the molecular surfaces of **1** - **3** are largely positive, the approximate similarity of σ_+^2 and σ_-^2 in each case indicates that the variation in the positive and negative potentials is roughly the same. In marked contrast, the positive potentials in **4** are clearly much greater in magnitude than are the negative, as well as more extensive; this is seen in Figure 3b and in the fact that $\sigma_+^2 \gg \sigma_-^2$.

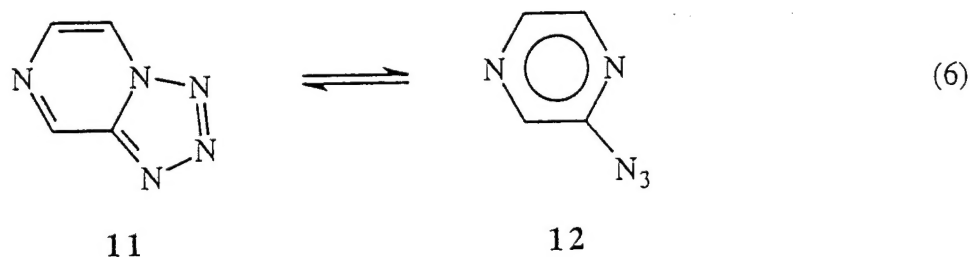
Discussion

The possibility of tetrazolo-azido tautomerism is well-established for nitrogen heterocyclic systems [5-12]; for **2** and **3** it is represented by eqs. (4) and (5):



The general experience has been that the tetrazolo tautomers appear to be favored by a high electronic density associated with the central heterocyclic ring and in particular with the nitrogen

that is common to both rings in the tetrazolo form [5-9]; thus, electron-withdrawing substituents tend to promote the azido tautomer. However environmental factors can be extremely important [5-12]; for example, the equilibrium shown in eq. (6) has been observed in chloroform and in trifluoroacetic acid solutions [6], but only **11** is present in the solid phase [31].



From our computed energies in Table 1, we obtain $\Delta E = 12.7$ kcal/mole for eq. (4) and $\Delta E = -5.2$ kcal/mole for eq. (5). Since we find **6** to be slightly more stable than **3** on a molecular level, the fact that **3** is the form that is observed in the solid phase [4] is presumably due to stabilization provided by crystal lattice interactions.

In seeking to understand the contrast between the equilibria in eqs. (4) and (5), wherein the former favors the tetrazole and the latter the azide, it is useful to look at the computed electrostatic potentials of the two azides, **5** and **6**; these are shown, on the molecular surfaces, in Figures 4 and 5. The minima associated with the nitrogens, both $V_{S,\min}(\text{N})$ and $V_{\min}(\text{N})$, are listed in Table 3.

An interesting feature of these results is the charge distribution in the azido group. Both Table 3 and Figures 4 and 5 show that the central nitrogen is positive in character, while the linking one is strongly negative; the outermost nitrogen is intermediate between these extremes. Thus, in terms of the resonance description of the azido group given in **13A** - **13C**, the dominant contributors appear to be **13A** and **13B**. This conclusion is consistent with the structural data in Table 1, as well as with earlier interpretations [32].

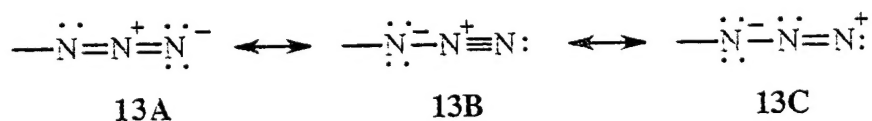
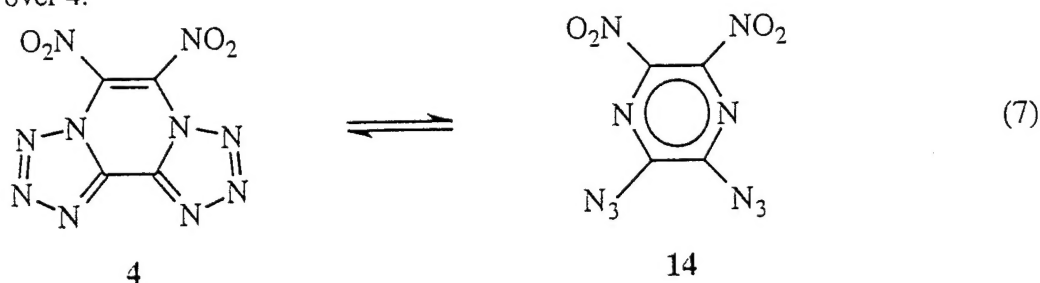


Table 3 also reveals the ring nitrogens in **5** to be more negative than in **6**. In this respect, therefore, our finding that the tetrazole is more favored energetically in eq. (4) than in eq. (5) is in agreement with the past experience mentioned earlier [5-9].

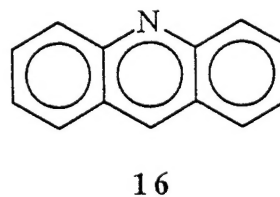
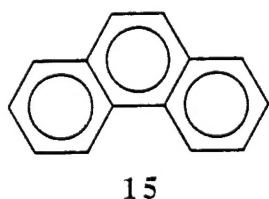
However this introduces a serious question concerning **4**, the dinitro derivative of **3**. We did verify that the optimized geometry of **4** corresponds to a true energy minimum; there are no imaginary vibrational frequencies [33]. On the other hand, since the azido tautomer **6** is already slightly more stable than the tetrazole **3**, and electron-withdrawing groups such as NO_2 promote

the formation of the azide, it may be that the azido tautomer **14** is considerably favored energetically over **4**:



We have accordingly computed an optimized geometry and energy for **14**, using the Gaussian 92/DFT procedure described earlier [22-24]. The resulting energy, -1000.37066 hartrees, yields $\Delta E = -27.4$ kcal/mole for eq. (7). This confirms that the introduction of nitro groups in **3** will be expected to shift the tautomeric equilibrium significantly toward the azide. This is unfortunate from the standpoint of an energetic material, because of the well-known proclivity of many azides for facile decomposition [32].

The density of a molecular crystal depends upon the mass and size of the molecule, and upon the crystalline structure and packing. It is interesting to compare **1** - **3** to phenanthrene (**15**) and acridine (**16**). The molecular weights of the first three are somewhat less than those of the last two, yet the densities of **1** - **3** are more than 30% greater than those of **15** and **16** [34]. Much of this difference can be attributed to the smaller volumes of **1** - **3** (Table 2), all of which are at least 25% less than the 201.4 \AA^3 of **15** and 199.3 \AA^3 of **16** [35].



This is fully consistent with the findings of Stine, who analyzed the crystal structures of more than 2000 organic compounds to obtain effective volumes for their constituent atoms in various bonding environments [36]. He concluded that, in general, high densities are promoted by maximizing the numbers of nitrogens and oxygens and minimizing the numbers of carbons and hydrogens.

Molecular interactions are also expected to play a role in determining the densities of organic compounds. We have found σ_{tot}^2 to be an effective measure of this, for crystal densities [25] as well as for a variety of other macroscopic properties, including critical constants, boiling points, heats of vaporization, partition coefficients and supercritical solubilities [18-21, 25]. Since density increases with σ_{tot}^2 [25], the large magnitudes of the latter property for **1** - **3**, greatly

exceeding the σ_{tot}^2 values of typical organic compounds (as pointed out above), are a second factor in the high densities of **1** - **3**, in addition to their relatively small sizes.

Summary

We suggest that the high densities found crystallographically for **1** - **3** can be attributed to their relatively small molecular volumes and the strong intermolecular attractions arising from the highly varying electrostatic potentials on their molecular surfaces. **3** and **4** can be involved in tautomeric equilibria with diazides, and in the gas phase, **3** is 5.2 kcal/mole more stable as the diazide, although in the crystal it exists only as the tetrazole. In the dinitro derivative of **3**, the energetic preference for the diazide tautomer is greatly enhanced, indicating that its usefulness as an energetic material is open to question.

Acknowledgement

We appreciate the financial support of the office of Naval Research through contract no. N00014-95-1-0028.

References

1. Kamlet, M. J.; Jacobs, S. J. *J. Chem. Phys.* **1968**, *48*, 23.
2. Hosmane, R. S.; Rossman, M. A.; Leonard, N. J. *J. Am. Chem. Soc.* **1982**, *104*, 5497.
3. Gilardi, R.; George, C.; Flippen-Anderson, J. L. Naval Research Laboratory, Annual Report to Office of Naval Research; Arlington, VA 22217, 1986.
4. Gilardi, R.; George, C.; Flippen-Anderson, J. L. Naval Research Laboratory, Annual Report to Office of Naval Research; Arlington, VA 22217, 1985.
5. Boyer, J. H.; Miller, E. J., Jr. *J. Am. Chem. Soc.* **1959**, *81*, 4671.
6. Wentrup, C. *Tetrahedron* **1970**, *26*, 4969.
7. Sasaki, T.; Kanematsu, K.; Murata, M. *J. Org. Chem.* **1971**, *36*, 446.
8. Tisler, M. *Synthesis* **1973**, 123.
9. Goodman, M. M.; Atwood, J. L.; Carlin, R.; Hunter, W.; Paudler, W. W. *J. Org. Chem.* **1976**, *41*, 2860.
10. Neunhoeffer, H. In *Comprehensive Heterocyclic Chemistry*; Boulton, A. J.; McKillop, A. Eds.; Pergamon: Oxford, 1984; Vol. 3, Part 2B; ch. 2.19.
11. Denisov, A. Y.; Krivopalov, V. P.; Mamatyuk, V. I.; Mamaev, V. P. *Magn. Reson. Chem.* **1988**, *26*, 42.
12. Krivopalov, V. P.; Baram, S. G.; Denisov, A. Y.; Mamatyuk, V. I. *Izv. Akad. Nauk., SSSR, Ser. Khim.* **1989**, *9*, 2002.
13. Politzer, P.; Truhlar, D. G. *Chemical Applications of Atomic and Molecular Electrostatic Potentials*; Plenum Press: New York, 1981.
14. Scrocco, E.; Tomasi, J. *Adv. Quant. Chem.* **1978**, *11*, 115.
15. Politzer, P.; Murray, J. S. In *Reviews in Computational Chemistry*; Lipkowitz, K. B.; Boyd, D. B. Eds.; VCH Publishers: New York, 1991; Vol. 2; ch. 7.
16. Bader, R. F. W.; Carroll, M. T.; Cheeseman, J. R.; Chang, C. *J. Am. Chem. Soc.* **1987**, *109*, 7968.
17. Brinck, T.; Murray, J. S.; Politzer, P. *Mol. Phys.* **1992**, *76*, 609.
18. Politzer, P.; Murray, J. S.; Lane, P.; Brinck, T. *J. Phys. Chem.* **1993**, *97*, 729.
19. Brinck, T.; Murray, J. S.; Politzer, P. *J. Org. Chem.* **1993**, *58*, 7070.
20. Murray, J. S.; Lane, P.; Brinck, T.; Paulsen, K.; Grice, M. E.; Politzer, P. *J. Phys. Chem.* **1993**, *97*, 9369.
21. Murray, J. S.; Brinck, T.; Lane, P.; Paulsen, K.; Politzer, P. *J. Mol. Struct. (Theochem)* **1994**, *307*, 55.
22. Frisch, M. J.; Trucks, G. W.; Schlegel, H. B.; Gill, P. M. W.; Johnson, B. G.; Wong, M. W.; Foresman, J. B.; Robb, M. A.; Head-Gordon, M.; Replogle, E. S.; Gomperts, R.;

- Andres, J. L.; Raghavachari, K.; Binkley, J. S.; Gonzalez, C.; Martin, R. L.; Fox, D. J.; DeFrees, D. J.; Baker, J.; Stewart, J. J. P.; Pople, J. A. GAUSSIAN 92/DFT, Gaussian, Inc.: Pittsburgh, PA, 1993.
23. Becke, A. D. *Phys. Rev. A* **1988**, *38*, 3098.
 24. Lee, C.; Yang, W.; Parr, R. G. *Phys. Rev. B* **1988**, *37*, 785.
 25. Murray, J. S.; Brinck, T.; Politzer, P. *Chem. Phys.* in press.
 26. Murray, J. S.; Lane, P.; Politzer, P. *Mol. Phys.* **1995**, *85*, 1.
 27. Politzer, P.; Murray, J. S.; Seminario, J. M.; Miller, R. S. *J. Mol. Struct. (Theochem)* **1992**, *262*, 155.
 28. Murray, J. S.; Seminario, J. M.; Politzer, P. *J. Mol. Struct. (Theochem)* **1989**, *187*, 95.
 29. Brinck, T.; Murray, J. S.; Politzer, P.; Carter, R. E. *J. Org. Chem.* **1991**, *56*, 2934.
 30. Murray, J. S.; Politzer, P. *J. Chem. Res.* **1992**, *S*, 110.
 31. Rutner, H.; Spierri, P. E. *J. Heterocyclic Chem.* **1966**, *3*, 435.
 32. Boyer, J. H.; Canter, F. C. *Chem. Rev.* **1954**, *54*, 1.
 33. Hehre, W. J.; Radom, L.; Schleyer, P. v. R.; Pople, J. A. *Ab Initio Molecular Orbital Theory*; Wiley-Interscience: New York, 1986.
 34. Dean, J. A. *Lange's Handbook of Chemistry*, 14th ed.; McGraw-Hill: New York, 1992.
 35. DeSalvo, M.; Miller, E.; Murray, J. S.; Politzer, P., unpublished work.
 36. Stine, J. R. In *Structure and Properties of Energetic Materials*; Liebenberg, D. H.; Armstrong, R. W.; Gilman, J. J. Eds.; Materials Research Society: Pittsburgh, 1993.

Figure Captions

- Figure 1. Calculated electrostatic potential on the molecular surface of 1. Monochrome ranges, in kcal/mole, are: dark gray for $V(r) > 35$; light gray for $V(r)$ from 35 to 0; white for negative values of $V(r)$.
- Figure 2. Calculated electrostatic potential on the molecular surface of 2. Monochrome ranges, in kcal/mole, are: dark gray for $V(r) > 35$; light gray for $V(r)$ from 35 to 0; white for negative values of $V(r)$.
- Figure 3. Calculated electrostatic potential on the molecular surface of: (a) 3 and (b) its dinitro derivative 4. Monochrome ranges, in kcal/mole, are: dark gray for $V(r) > 35$; light gray for $V(r)$ from 35 to 0; white for negative values of $V(r)$.
- Figure. 4. Calculated electrostatic potential on the molecular surface of 5. Monochrome ranges, in kcal/mole, are: dark gray for $V(r) > 15$; light gray for $V(r)$ from 15 to 0; white for negative values of $V(r)$.
- Figure. 5. Calculated electrostatic potential on the molecular surface of 6. Monochrome ranges, in kcal/mole, are: dark gray for $V(r) > 15$; light gray for $V(r)$ from 15 to 0; white for negative values of $V(r)$.

Table 1. DF/B-LYP/6-31G** calculated bond distances and energies and experimentally-determined bond distances.^a

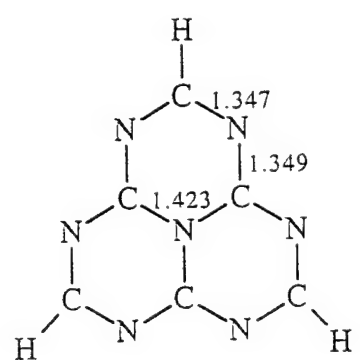
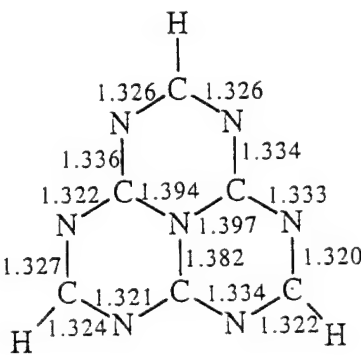
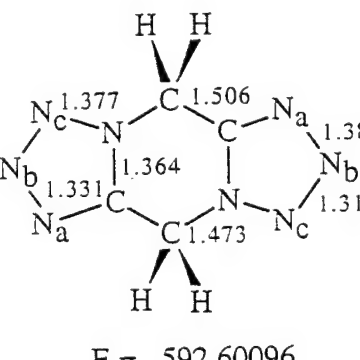
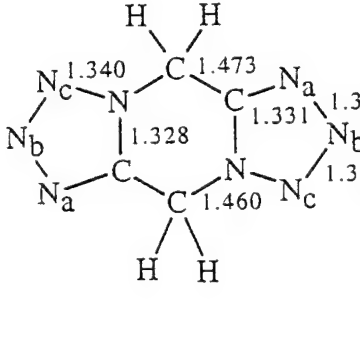
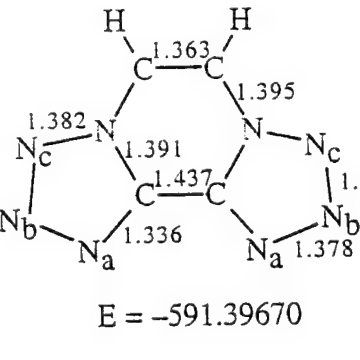
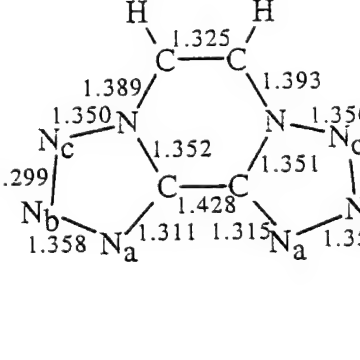
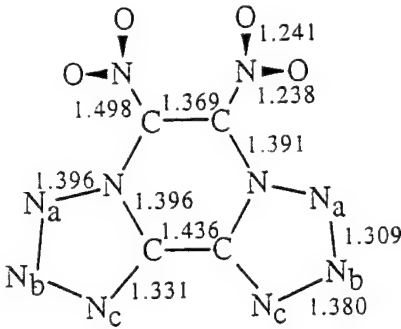
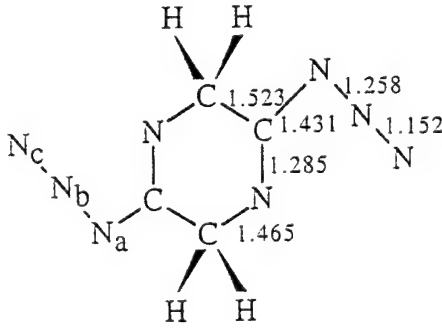
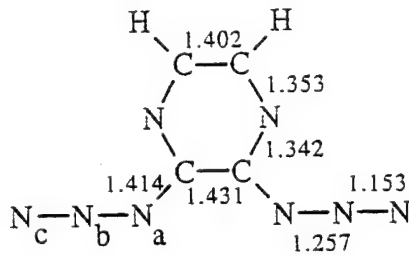
	calculated bond distances (Å) and energy (hartrees)	experimentally-determined bond distances ^a (Å)
1	 <p>E = -613.55104</p>	 <p>E = -613.55104</p>
2	 <p>E = -592.60096</p>	 <p>E = -592.60096</p>
3	 <p>E = -591.39670</p>	 <p>E = -591.39670</p>

Table 1. DF/B-LYP/6-31G** calculated bond distances and energies and experimentally-determined bond distances (continued).^a

	calculated bond distances (Å) and energy (hartrees)	experimentally-determined bond distances ^a (Å)
4	 <p>$E = -1000.32701$</p>	-----
5	 <p>$E = -592.58066$</p>	-----
6	 <p>$E = -591.40491$</p>	-----

^aThe experimental data for 1, 2 and 3 are from references 2 - 4, respectively.

Table 2. Calculated and experimental properties of 1 - 4.^a

Molecule	density	surface area	volume ^b	V _{S,max}	V _{S,min(N)}	V _{min(N)}	Π	σ ₊ ²	σ ₋ ²	σ _{tot} ²
1	1.689 ^c	163.9	145.4	52.2	-43.2	-78.1	21.2	181.7	172.3	354.0
2	1.715 ^d	162.0	141.7	53.7	N _a : -38.9 N _b : -42.8 N _c : -28.5	N _a : -72.0 N _b : -70.9 N _c : -52.3	23.4	111.9	126.3	238.2
3	1.674 ^e	153.3	133.7	50.2	N _a : -25.4 N _b : -41.4 N _c : -44.0	N _a : -47.7 N _b : -68.8 N _c : -73.3	24.7	130.6	137.0	267.6
4	----	200.0	174.3	72.0	N _a : -18.6 N _b : -31.3 N _c : -32.2	N _a : -48.6 N _b : -54.9 N _c : -57.9	21.6	358.6	64.3	422.9

^aUnits: density, g/cm³; area, Å²; volume, Å³; all potentials and Π, kcal/mole; σ₊², σ₋² and σ_{tot}²

(kcal/mole)². The labeling of the nitrogens follows Table 1.

^bReference 36.

^cReference 2.

^dReference 3.

^eReference 4.

Table 3. Most negative electrostatic potentials, $V_{S,min}(N)$ and $V_{min}(N)$, associated with the nitrogens in the azides **5** and **6**.^a

Molecule	$V_{S,min}(N)$, kcal/mole	$V_{min}(N)$, kcal/mole
5	N _{ring} : -32.6	N _{ring} : -72.2
	N _a : -29.3	N _a : -57.9
	N _b : none found	N _b : none found
	N _c : -19.7	N _c : -28.0
6	N _{ring} : -28.6	N _{ring} : -65.9
	N _a : -49.2 ^b	N _a : -68.3
	N _b : none found	N _b : none found
	N _c : -19.9	N _c : -28.1

^aThe labeling of the nitrogens follows Table 1.

^bThe negative surface region associated with each N_a overlaps that of the other, and there is only one local minimum.

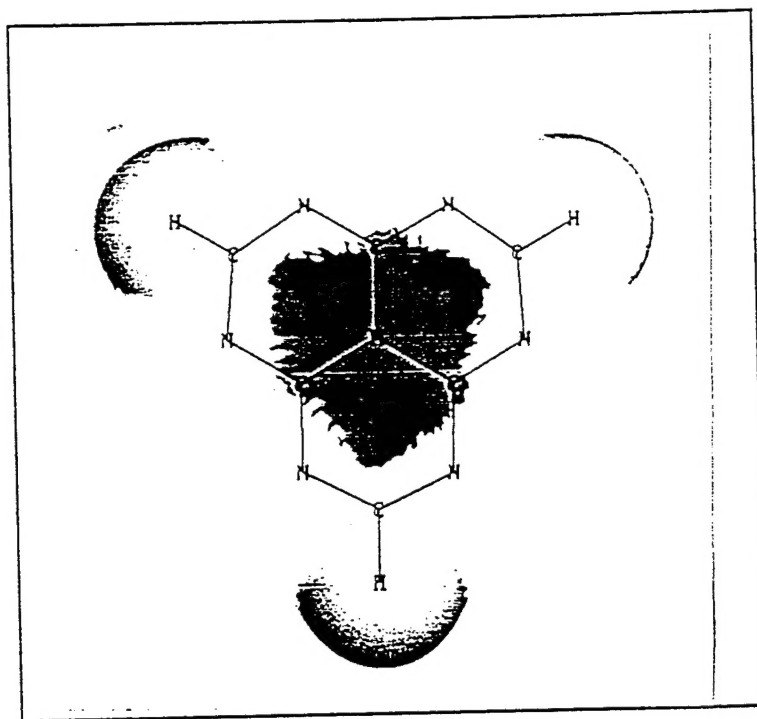


Figure 1. Calculated electrostatic potential on the molecular surface of 1. Monochrome ranges, in kcal/mole, are: dark gray for $V(r) > 35$; light gray for $V(r)$ from 35 to 0; white for negative values of $V(r)$.

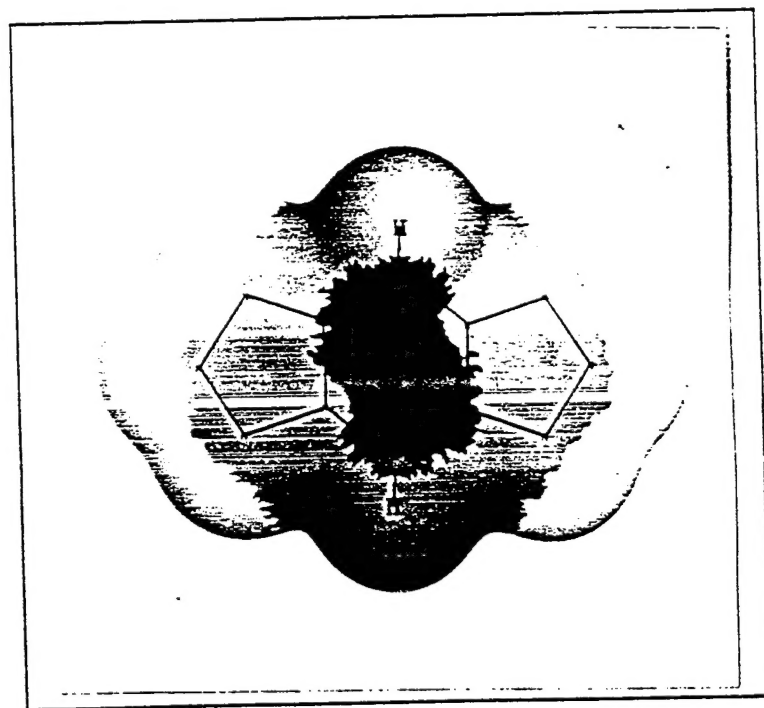
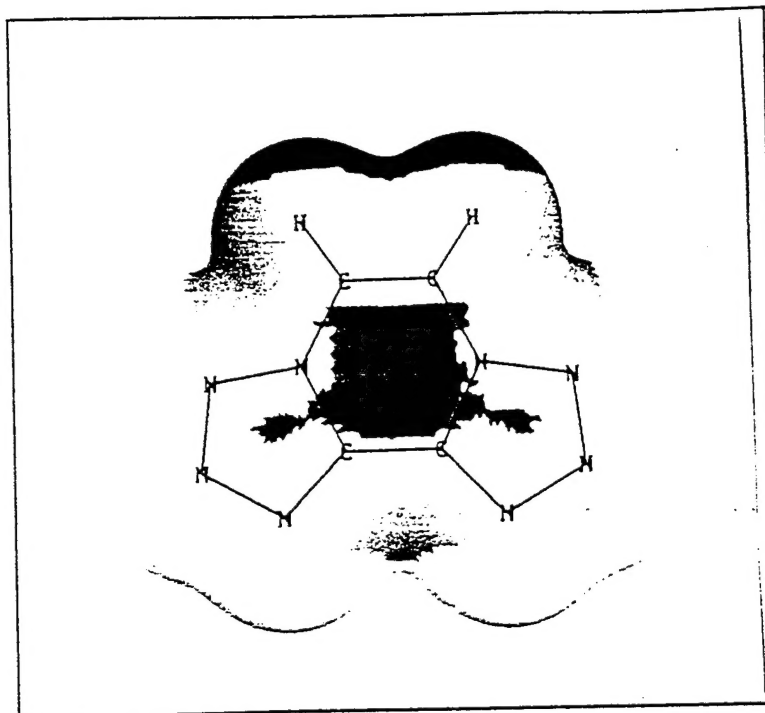


Figure 2. Calculated electrostatic potential on the molecular surface of 2. Monochrome ranges, in kcal/mole, are: dark gray for $V(r) > 35$; light gray for $V(r)$ from 35 to 0; white for negative values of $V(r)$.

(a)



(b)

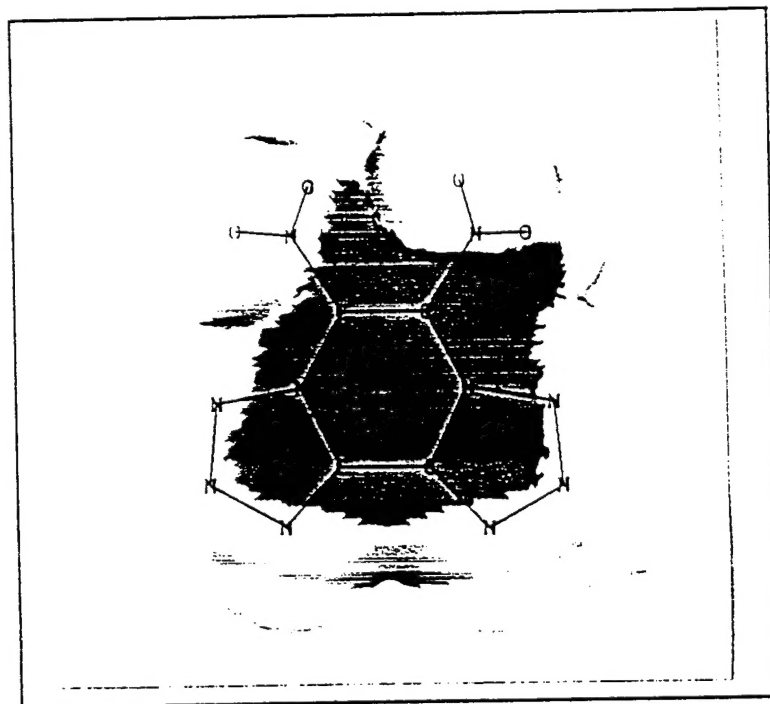


Figure 3. Calculated electrostatic potential on the molecular surface of: (a) 3 and (b) its dinitro derivative 4. Monochrome ranges, in kcal/mole, are: dark gray for $V(r) > 35$; light gray for $V(r)$ from 35 to 0; white for negative values of $V(r)$.

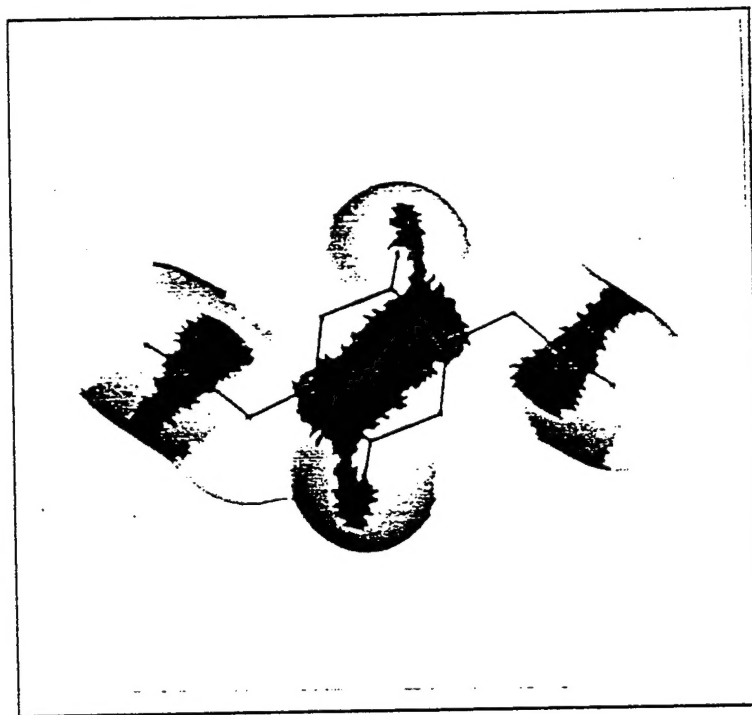


Figure. 4. Calculated electrostatic potential on the molecular surface of 5. Monochrome ranges, in kcal/mole, are: dark gray for $V(r) > 15$; light gray for $V(r)$ from 15 to 0; white for negative values of $V(r)$.

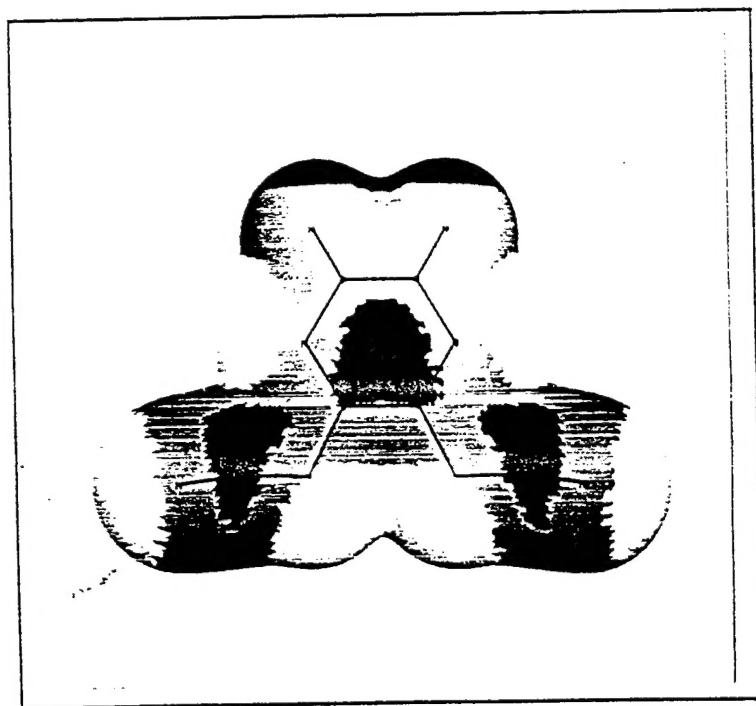


Figure. 5. Calculated electrostatic potential on the molecular surface of 6. Monochrome ranges, in kcal/mole, are: dark gray for $V(r) > 15$; light gray for $V(r)$ from 15 to 0; white for negative values of $V(r)$.